JOURNAL OF THE AMERICAN WATER RESOURCES ASSOCIATION
Vol. 52, No. 5 AMERICAN WATER RESOURCES ASSOCIATION October 2016

RECONSTRUCTIONS OF COLUMBIA RIVER STREAMFLOW FROM TREE-RING CHRONOLOGIES IN THE PACIFIC NORTHWEST, USA[1]

Jeremy S. Littell, Gregory T. Pederson, Stephen T. Gray, Michael Tjoelker, Alan F. Hamlet, and Connie A. Woodhouse[2]

ABSTRACT: We developed Columbia River streamflow reconstructions using a network of existing, new, and updated tree-ring records sensitive to the main climatic factors governing discharge. Reconstruction quality is enhanced by incorporating tree-ring chronologies where high snowpack limits growth, which better represent the contribution of cool-season precipitation to flow than chronologies from trees positively sensitive to hydroclimate alone. The best performing reconstruction (back to 1609 CE) explains 59% of the historical variability and the longest reconstruction (back to 1502 CE) explains 52% of the variability. Droughts similar to the high-intensity, long-duration low flows observed during the 1920s and 1940s are rare, but occurred in the early 1500s and 1630s-1640s. The lowest Columbia flow events appear to be reflected in chronologies both positively and negatively related to streamflow, implying low snowpack and possibly low warm-season precipitation. High flows of magnitudes observed in the instrumental record appear to have been relatively common, and high flows from the 1680s to 1740s exceeded the magnitude and duration of observed wet periods in the late-19th and 20th Century. Comparisons between the Columbia River reconstructions and future projections of streamflow derived from global climate and hydrologic models show the potential for increased hydrologic variability, which could present challenges for managing water in the face of competing demands.

(KEY TERMS: climate variability; climate change; dendrochronology; drought; snow hydrology; paleoclimate; streamflow; water supply.)

Littell, Jeremy S., Gregory T. Pederson, Stephen T. Gray, Michael Tjoelker, Alan F. Hamlet, and Connie A Woodhouse, 2016. Reconstructions of Columbia River Streamflow from Tree-Ring Chronologies in the Pacific Northwest, USA. *Journal of the American Water Resources Association* (JAWRA) 52(5):1121-1141. DOI: 10.1111/1752-1688.12442

INTRODUCTION

The Columbia River drains approximately 75% of the Pacific Northwest (PNW) and accounts for 55-56% of the total runoff from the region (Miles *et al.*, 2000). The PNW relies on Columbia River water for hydropower, transportation, municipal water supply, agricultural irrigation, and fish habitat. The water resources management system in the Columbia River

[1]Paper No. JAWRA-15-0050-P of the *Journal of the American Water Resources Association* (JAWRA). Received April 16, 2015; accepted May 25, 2016.

[2]Research Ecologist (Littell) and Director (Gray), DOI Alaska Climate Science Center, United States Geological Survey, 4210 University Drive, Anchorage, Alaska 99508; Research Ecologist (Pederson), Northern Rocky Mountain Science Center, United States Geological Survey, Bozeman, Montana 59715; Content Specialist (Tjoelker), FRAMES, College of Natural Resources, University of Idaho, Moscow, Idaho 83844; Assistant Professor (Hamlet), Department of Civil and Environmental Engineering and Earth Sciences, University of Notre Dame, Notre Dame, Indiana 46556; and Professor (Woodhouse), School of Geography and Development, University of Arizona, Tucson, Arizona 87521 (E-Mail/Littell: jlittell@usgs.gov).

Basin is sensitive to climatic variability (Miles *et al.*, 2000), in part because reservoir storage capacity is limited to around 30% of annual flow (Bonneville Power Administration, Bureau of Reclamation and U.S. Army Corps of Engineers, 1995). Knowledge of the plausible variations in streamflow is therefore key to future strategic planning because economic activity and individual livelihoods are related to water availability (Lee, 1993; NRC, 1996). The historical record (A.G. Crook Company, 1993; Naik and Jay, 2005) and modeling (Hamlet *et al.*, 2013) indicate that the Columbia River Basin experienced drought-prone periods between about 1920 and 1941 (four separate three-year periods below median flow, 10 years below the 25th percentile including three consecutive years below the 10th percentile) and, more recently, between 2001 and 2005. Anomalously wet periods occurred in the late 1940s until about 1956 and between 1995 and 2000. However, in most cases, interannual variability punctuates these events with anomalous years of opposite sign; that is, wet years can occur during drought-prone periods and dry years during wetter periods.

Instrumental climate records from the PNW show that hydrologic "drought" is not simply a lack of water on an annual basis, but can be either a lack of winter precipitation stored as snowpack (Miles *et al.*, 2000; Bumbaco and Mote, 2010), or a lack of summer precipitation — both of which differentially affect streamflow. For example, Maurer *et al.* (2004) used the Variable Infiltration Capacity (VIC) distributed hydrologic model to demonstrate summertime (June to August — JJA) streamflow in the PNW was variably dependent on spring (March to May — MAM) snowmelt runoff and a combination of summer precipitation and late melting snow from year to year. Figure 1 shows the relationships between annual Columbia River streamflow and both warm- (April to September — AMJJAS) and cool-season (October to March — ONDJFM) precipitation, indicating a significant relationship only between cool-season precipitation and annual streamflow during the instrumental record.

Paleoproxy reconstructions of hydroclimate can extend records of river flow prior to historical gaged observations (e.g., Smith and Stockton, 1981; Cook and Jacoby, 1983; Meko *et al.*, 2001; Graumlich *et al.*, 2003; Gedalof *et al.*, 2004; Woodhouse *et al.*, 2006). Multicentennial to millennial streamflow reconstructions are particularly useful in documenting the long-term variability in streamflow prior to gaged records, and usually demonstrate an increased range of streamflow volumes at interannual to multidecadal time scales compared to the historical record (Jain *et al.*, 2002; Woodhouse *et al.*, 2006; Meko *et al.*, 2007). The extended range of natural variability in hydroclimatic reconstructions is valuable for understanding baseline risks of protracted (10-50+ years) high- and low-flow events providing direct implications for water resource management and planning today (Woodhouse and Lukas, 2006a, b and Rice *et al.*, 2009). When used in conjunction with climatic (Ault *et al.*, 2013) and hydrologic models (e.g., Gray and McCabe, 2010; Lutz *et al.*, 2012), pre-gage-record variability may provide improved accuracy of present and future climate change related risk to water resources (Hidalgo *et al.*, 2009; Ault *et al.*, 2013).

A previous reconstruction of Columbia River flows by Gedalof *et al.* (2004) extended back to 1750 CE and showed periods of sustained low flows in the late 1770s, early 1800s, 1840s, late 1880s, early 1920s, and 1930s. They described the 1840s as possibly exceeding the magnitude and duration of the back-to-

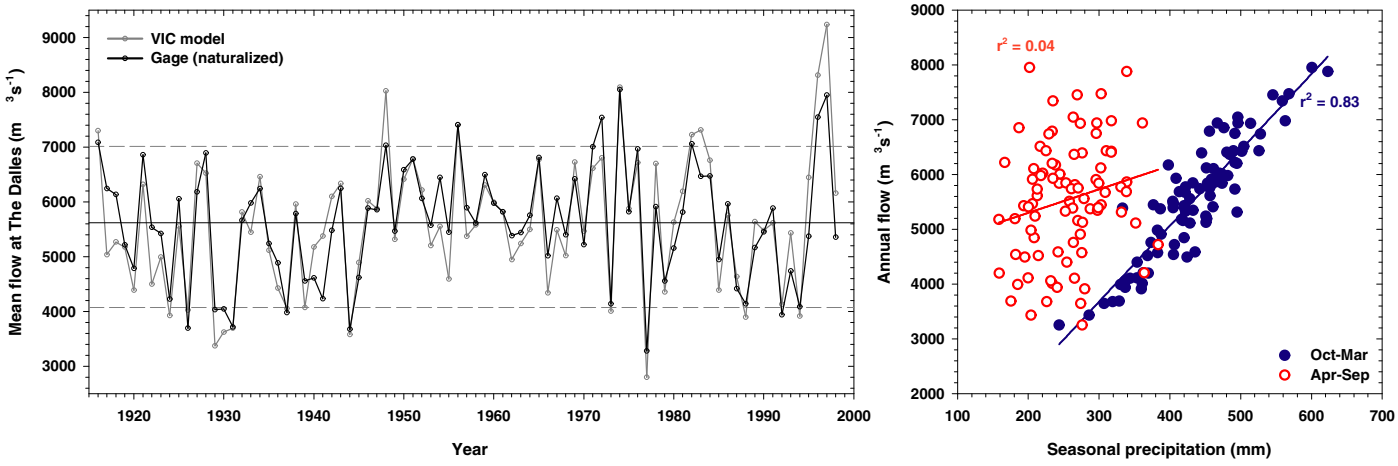

FIGURE 1. Left: Mean Water Year Flow in the Columbia River at The Dalles, 1916-1998 Naturalized USGS Gage and Modeled Variable Infiltration Capacity (VIC) at The Dalles, Oregon. Right: Relationship between naturalized streamflow and VIC basin-average gridded (1) cool-season (Oct.-Mar.) precipitation (solid, $r^2 = 0.83$) and (2) warm-season (Apr.-Sep.) precipitation (open, $r^2 = 0.04$).

back early 20th Century droughts (i.e., 1920s-1940s). Wise (2010) reconstructed upper Snake River (the Columbia's major southern tributary) streamflow, and showed the drought of the 1620s-1640s was similar in duration but greater intensity than the 1920s and 1930s drought. Malevich *et al.* (2013) reconstructed water-year precipitation for Klamath River drainage, a basin located to the south of the Columbia, and Meko *et al.* (2014) developed a streamflow reconstruction for the Klamath River at Keno, Oregon (OR). They describe a severe drought in the 17th Century and suggest it was of similar magnitude to the early-20th Century event, but the 11th and late 12th Century droughts were more severe than any in the instrumental period. Lutz *et al.* (2012) developed a cool-season precipitation and warm-season streamflow reconstruction for the Yakima River (a Columbia tributary in the eastern Cascades) back to 1614 CE that also indicates low flows during the 17th Century and 19th Century of comparable severity to the early 20th Century. Given the economic importance of water in the Columbia River Basin, the severe droughts indicated in these regional streamflow reconstructions illustrate the need to develop an updated Columbia streamflow reconstruction as far back in time as the proxy record will permit to better estimate the intrinsic, climatically forced variability in the basin's water resources. Herein, we improve and extend previous work by developing a new Columbia River flow reconstruction that more fully incorporates the major seasonal controls on hydrologic variability, and integrates a large number of new and updated regional tree-ring records.

To date, reconstructions of streamflow in the western United States (U.S.) have relied primarily on chronologies developed with water-limited trees (Meko *et al.*, 1995, 2001, 2014; Graumlich *et al.*, 2003; Woodhouse *et al.*, 2006; Wise, 2010). The seasonality of water limitation varies with species and climate (Wettstein *et al.*, 2011; St. George and Ault, 2014), but streamflows are affected by water availability in both winter and summer in much of the west. In the PNW, tree growth in some chronologies is negatively correlated with snowpack (e.g., Peterson and Peterson, 2001) because the duration of snowpack limits the growing season length. Of the PNW hydroclimate reconstructions described above, only the Gedalof *et al.* (2004) reconstruction attempted to include tree-ring chronologies directly limited by snowpack within a streamflow reconstruction, although they screened for chronologies negatively associated with annual Palmer Drought Severity Index (PDSI) as an indirect approach to include snowpack sensitivity. In Pederson *et al.* (2011), a network of snow-sensitive tree-ring proxies along the American Cordillera was developed by screening chronologies directly against April 1st Snow Water Equivalent (SWE) measurements to produce snowpack reconstructions in watersheds of the American West. The approach demonstrated how both water-limited growth suppression and snowpack-induced growth suppression (i.e., snowpack limited) could be used in tandem to accurately reconstruct basin-level snowpack histories. In this study, we use existing, updated, and new "water-limited" and "snowpack-limited" tree-ring chronologies to reconstruct annual Columbia River streamflow at The Dalles, OR. We then compare the new streamflow reconstructions for the Columbia River to existing hydroclimatic reconstructions from the surrounding region and results from global climate and hydrologic models to assess potential future changes in water resources compared to the river's historical range of variability.

METHODS

To reconstruct Columbia streamflow, we (1) obtained naturalized streamflow data at The Dalles, OR, and gridded climate data for the Columbia Basin region; (2) obtained and screened existing and new chronologies for fidelity to Columbia streamflow; (3) used the screened tree-ring chronologies as predictors in multiple regression models and reconstructions of Columbia flow; and (4) evaluated the quality of each reconstruction. As a variant of (3), we also used Empirical Orthogonal Function/Principal Components analysis (EOF/PC, e.g., Preisendorfer, 1988) to derive leading modes of variability from the chronology networks that were then used to produce reconstructions based on the spatial patterns (and their principal component time series) explaining the most variance over the entire network of tree-ring chronologies.

Streamflow Data

For this work, we used the streamflow gage at The Dalles, OR, for two reasons. First, the gage integrates flow from the majority of the Columbia River Basin at a single point. Second, past studies have constructed careful analyses of historical and naturalized flows over a long period, which is a key consideration for calibrating reconstructions from paleoproxies, particularly in a regional climate with strong decadal variability. Naturalized annual flow at The Dalles, OR (USGS gage 14105700), has been estimated between 1858 and 1998 (A.G. Crook Company, 1993; Naik and Jay, 2005). From 1858 to 1877, railroad workers measured spring peak flow using stage height, and annual

flows have been reconstructed from these records using regression relationships between annual flow and observed peak flow. From 1878 to 1928, naturalized monthly flow was estimated by Naik and Jay (2005) from gaged daily observations, and from 1928 to 1998 naturalized monthly flow was estimated by A.G. Crook Company (1993 and updates). The VIC hydrologic model was used to produce flow estimates from observed precipitation and temperature for the period 1916-2003 (Hamlet *et al.*, 2005, 2007), allowing a model-based verification of the naturalized flows. We compared the naturalized flow estimates and the VIC modeled flow estimates for the common period (water years 1916-1998). For this portion of the record, the estimates closely match ($r = 0.91$, Figure 1), so we chose to use 1916-1998 naturalized flow as the calibration data (including both the Naik and Jay and A.G. Crook Company estimates) for reconstruction. The naturalized flow therefore is a calculated estimate, but compares favorably with simulations from a physically based hydrology model and also measured observations prior to the construction of major dams (prior to about 1940).

Figure 1 shows the estimated naturalized annual gage record from 1916 to 1998. We chose not to use additional naturalized gage records available from 1878 to 1915 (Naik and Jay, 2005) because we could not validate these earlier records against other sources of data or determine whether the flows were consistent with post-1928 naturalized data (A.G. Crook Company, 1993).

Hydroclimatic Data

We used interpolated, gridded monthly climate data (temperature and precipitation) and derived hydroclimatic variables [snowpack, soil moisture, potential evapotranspiration (PET), actual evapotranspiration, and base flow] from the VIC model (Elsner *et al.*, 2010; Hamlet *et al.*, 2013; after Hamlet *et al.*, 2005, 2007) to better understand the climatic controls on both Columbia River streamflow and tree growth for the calibration period 1916-1998. Briefly, we generated a dataset similar to that in Elsner *et al.* (2010, 1/16th degree VIC hydrologic output), but for the combined greater Northwest spanning the domain of the greater Columbia Basin (~39-53° N latitude, ~−123° to −105° W longitude), including coastal Washington and Oregon as well as the Columbia, upper Colorado, and upper Missouri River Basins (Littell *et al.*, 2011 online). This dataset follows Hamlet and Lettenmaier (2005), who used daily climate data from the NOAA Cooperative Observer Program Network integrated with monthly U.S. Historical Climate Network (Menne *et al.*, 2009) weather station data to interpolate gridded climate at 1/16th degree (6 km^2 at ~45°N). They further bias corrected the final dataset using monthly Parameter-elevation Relationships on Independent Slopes Model (PRISM) (Daly *et al.*, 1994, 2008) climatologies for each 1/16th degree cell. Elsner *et al.* (2010) used the 1/16th degree gridded climate data to drive the VIC hydrologic model and develop the final derived hydroclimatic and streamflow data (see Elsner *et al.*, 2010; Hamlet *et al.*, 2013). These data verify that Columbia Basin streamflow is predominantly controlled by cool season (Oct-Mar) precipitation entrained in snowpack (Maurer *et al.*, 2004; Elsner *et al.*, 2010) (Figure 1).

Tree-Ring Data

All publicly available and collaborator-provided chronologies in a domain containing the Columbia Basin were initially considered (39°-55° N latitude, from the Pacific coast to −104.5° W longitude, see Figure 2). As of 2012, this included 652 chronologies: 501 from the International Tree-Ring Data Bank (ITRDB, Accessed December 2012, http://www.ncdc.noaa.gov/data-access/paleoclimatology-data/datasets/tree-ring) for which raw ring widths were available; 124 Douglas-fir chronologies (Littell *et al.*, 2008); 3 Alaska Yellow Cedar (*Callitropsis/Chamaecyparis nootkatensis*) chronologies from Washington (Robertson, 2011); and 24 unpublished chronologies. In addition, we updated nine ITRDB chronologies that exhibited high correlation with Columbia River flows in preliminary screening (see Supporting Information).

Chronologies were removed if they did not span at least the period from 1650 to 1979 CE, or if some aspect of their collection or processing might negatively impact their suitability for use in climatic reconstructions such as chronologies collected to examine growth impacts of periodic insect infestation (e.g., Speer *et al.*, 2001);. The 1650 starting date was selected to optimize the number of potential chronologies, sample depth within chronologies, and potential reconstruction length. The 1979 end date allowed the incorporation of 1977 low flows into the calibration/screening process while capturing the many chronologies developed across the PNW between 1977 and 1985. This process resulted in 282 potential predictor chronologies (Figure 2).

For chronologies from Littell *et al.* (2008) and chronologies developed for this project and Pederson *et al.* (2011), all rings were measured and all samples visually crossdated for marker years using the "list method" (Yamaguchi, 1991) and all chronologies (including those from the ITRDB) were checked with COFECHA (Holmes, 1999). The program ARSTAN (versions 40C and 44, after Cook, 1985; Cook and

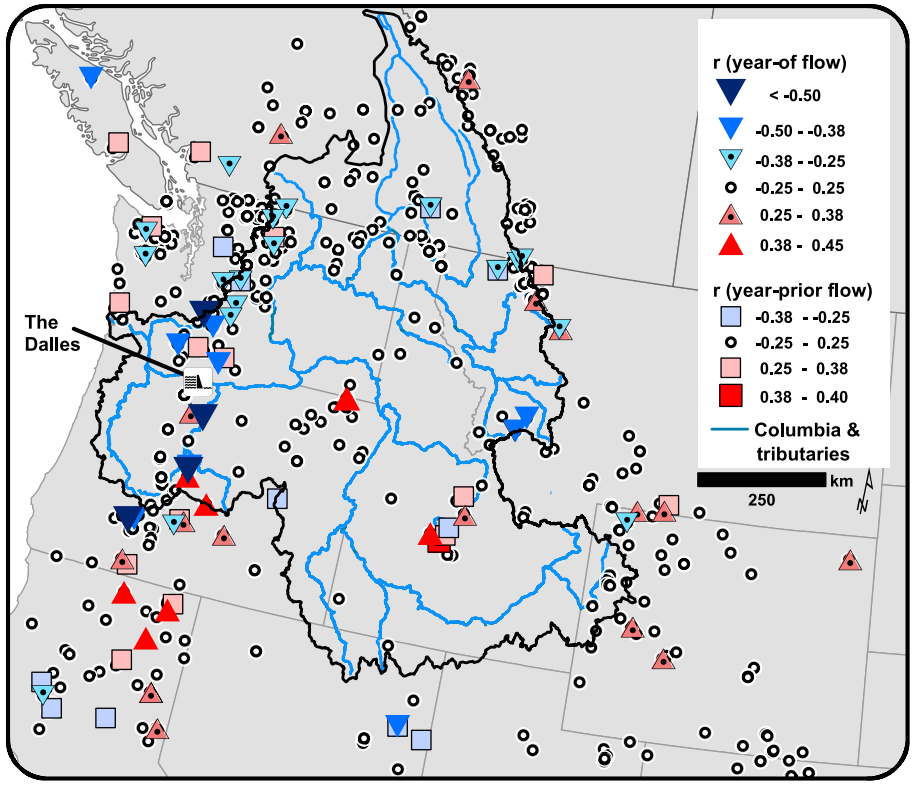

FIGURE 2. Chronologies Available and Screened Chronologies Considered for Reconstructions as Potential Streamflow Proxies Including Those Retained for Empirical Orthogonal Function/Principal Components (EOF/PC) Analysis. Filled symbols indicate correlation magnitude for chronologies significantly correlated with Columbia River flow (1916-1979). White dots indicate available but excluded chronologies. The Columbia River Basin boundary (dark gray line) and major river channels (blue lines) are shown for reference

Holmes, 1999) was used to standardize all chronologies (those from the ITRDB and those developed for this project). Initially either a negative exponential curve or negative linear trend was fit through the measured ring-width series. If either of the first two detrending equations did not provide satisfactory growth curve fit, a mean line or a cubic spline two thirds the length of the series was selected for use. To reduce the artificial inflation of variance due to decreasing sample size, we opted to stabilize variance (e.g., Briffa, 1995) and calculated the mean chronology as the weighted robust mean of the detrended series.

Pearson correlation coefficients were used to screen the 282 standard chronologies against historical (1916-1979) Columbia River streamflow. To account for the possibility that lags in physiological growth responses might cause some chronologies to have their strongest expressed relationship with climate (and thus streamflow) in the previous year, we also compared all chronologies to streamflow the year prior. Significantly ($|r|$ 0.246, $n = 64$, two tailed $p(t) = 0.05$) correlated chronologies were retained as a pool of possible streamflow proxies for reconstructions (Figure 2).

The climatic sensitivity (season and variable) of each chronology retained for potential use in a Columbia River flow reconstruction was further assessed using the VIC hydroclimatic data. Correlations were calculated between the standard chronologies and simulated hydroclimatic variables for the grid cells in which the chronologies were located. The seasonal climate correlations included: summer (Jun-Aug) precipitation, cool-season (Oct-Mar) precipitation, May 1 SWE, warm-season (Apr-Sep) PET, and warm-season (Apr-Sep) water balance deficit (potential minus actual evapotranspiration — PET-AET).

Estimating Streamflow from Tree-Ring Proxies

Two methods were used to reconstruct streamflow from the pool of potential predictor tree-ring chronologies. First, tree-ring chronologies were used directly as predictors in a stepwise multiple-linear regression model of streamflow. Second, an EOF/PC analysis was used to determine the dominant modes of variability in the network of tree-ring chronologies with the resulting PC time series applied as potential predictors in a multiple regression model of streamflow.

Multiple-Linear Regression Model of Streamflow

A multiple-linear regression reconstruction with individual chronologies as candidate predictors was developed using a forward stepwise selection procedure. The highest magnitude correlation predictor was entered first, regardless of sign, and so on until model construction stopped given the parameters below. We did this to avoid potential spuriousness associated with a predictor pool exceeding the number of observations. Candidate predictors were used in the model at $p(F) < 0.05$ and were retained if $p(F) < 0.10$ (as in Woodhouse *et al.*, 2006); order was determined by absolute value of magnitude of F. Significant predictors were added until the reduction in error statistic (RE, e.g., Fritts, 1976; equivalent to Nash-Sutcliffe efficiency index) could not be further improved and retained if the variance inflation factor (VIF, Neter *et al.*, 1996) statistics for each predictor remained below 3.0, indicating low potential problems with multicollinearity. This approach could result in predictors retained at $0.10 > p(F) > 0.05$. This procedure was performed twice, first on the pool of chronologies extending back to at least 1650 ($n = 82$) and then again on the pool of chronologies extending back past 1550 ($n = 61$).

Chronology Network EOF/PC Analysis

All screened potential predictor chronologies were used in EOF/PC analysis to derive coherent common signals among the chronologies significantly correlated with historical flow. Specifically, a singular value decomposition of the centered (e.g., Preisendorfer, 1988) standardized chronologies was performed. We modified methods described in Hidalgo *et al.* (2000), Meko *et al.* (2001), Gedalof *et al.* (2004), Woodhouse *et al.* (2006), and Meko *et al.* (2007) where principal components analysis (PCA) was used to reduce the dimensionality of the dataset and provide orthogonal, uncorrelated predictors of streamflow. In both the Hidalgo *et al.* (2000) and Woodhouse *et al.* (2006) approaches to PCA, the primary goal of the analysis was to capture the common signal with a positive relationship to streamflow (i.e., same sign correlation) in a network of tree-ring chronologies. Gedalof *et al.* (2004) accounted for the cool-season contribution further by screening available chronologies for those chronologies both positively and negatively correlated with PDSI, using PCA to separate the different responses into orthogonal PCs. There are, however, both ecological and statistical reasons to separate the effects of climate on tree growth into separate PCA analyses, each with hierarchical orthogonal modes. Two different growth-limiting mechanisms account for much of the proxy sensitivity to streamflow — cool season precipitation limitation of high elevation tree growth (snow limited) and cool-season and/or warm-season precipitation facilitation of lower elevation tree growth (water limited). Due to differences in the seasonal timing and the mechanism of these limitations, the proxy relationships with streamflow cannot be assumed to follow a hierarchy of variance that results in orthogonal modes of variability.

To preserve the different seasonal information in the set of chronologies, we used the methods employed in Lutz *et al.* (2012). We attempted to preserve different modes of cool-season and warm-season hydroclimatic variability by carrying out four separate EOF/PC analyses on the common analysis period (1650-1979) for standard chronologies (i.e., not residual or ARSTAN) that were (1) negatively and (2) positively correlated with water-year streamflow in the year of growth and, independently, for chronologies that were (3) negatively and (4) positively lag-1 autocorrelated with streamflow (growth in year following climate). Standard chronologies were used as input to the EOF/PC process because we argue that the coherent variation among chronologies at even multidecadal time scales is mostly climatic in nature in the PNW (Gedalof and Smith, 2001; Peterson and Peterson, 2001; Wettstein *et al.*, 2011) and therefore should be retained when it is held in common among chronologies. Because the sign of the first EOF/PC pair is arbitrary and can vary with computational methodology, we checked the loadings of the chronologies on each leading PC, and if all were negative, we inverted the sign of the PC time series to retain its correlation with streamflow when used as a predictor time series in regression. Within each EOF/PC analysis, we used the criterion proposed by North *et al.* (1982) with modification proposed by Bretherton *et al.* (1992) for autocorrelated time series to decide which PC time series to retain as independent predictors. In short, this method estimates which eigenvalues are statistically distinct from each other, but considers the "true" degrees of freedom in the time series given its autocorrelation. We retained all PCs distinct from each other as candidate predictors and rejected the rest.

Streamflow Reconstruction from EOF/PC Analysis

The retained PC time series of the four dominant modes of tree-ring response (cool-season precipitation limited, cool or warm-season precipitation enhanced, and these two modes lagged one year) were used as potential predictors in a regression model of observed (1916-1980) Columbia streamflow.

Again, a forward stepwise selection approach to regression model construction was employed, except with preference for leading mode PC time series. Specifically, year-of-correlation predictors were entered preferentially (e.g., PC1 snow limited, PC1 water limited, PC2 snow limited, and so on) with subsequent partiality for lower order modes and leading predictors (e.g., PC3 snow limited, PC3 lead1 water limited). Interaction terms were not considered, and the resulting calibrated regression model was used to develop a Columbia River streamflow reconstruction.

Streamflow Reconstruction Cross-Validation and Verification

Model robustness was assessed using two forms of cross-validation: the *PRESS* statistic (Neter *et al.*, 1996; after Allen, 1971) and split-sample tests (i.e., splitting the historical period and recomputing the calibrated regression model parameters from one subsample and validating the resulting model using the other subsample). Several regression diagnostic tests were used to assess and validate the reconstructions. To estimate the magnitude of the prediction error for the validation period, we computed the root mean squared error of validation ($RMSE_v$) and used $\pm 2*RMSE_v$ to estimate the 5th and 95th percentile confidence limits for the reconstructed flows. RE was used to measure the skill of the regression models, defined as their accuracy relative to a prediction based on no knowledge (i.e., the mean). Residual and quantile normality plots were examined to verify the assumption that residuals were normally distributed.

Examining the Hydroclimatic Features of Reconstructed Streamflow

A hybrid (1502-1983) reconstruction of the two reconstructions developed using direct regression of chronologies was assembled by rescaling the resulting 1502-1608 portion of the longer reconstruction to match the mean and variance of the shorter, more skillful, and better replicated 1609 reconstruction and appending the earlier years to the 1609 reconstruction. The hydroclimatic features of this extended reconstruction were then evaluated by calculating quantiles for each reconstructed water year. We then plotted the runs of years exceeding percentiles indicating low (less than 49th percentile, less than 25th percentile, and less than 10th percentile) and high (greater than 51st percentile, greater than 75th percentile, and greater than 90th percentile) flows to assess the duration and magnitude of high- and low-flow events.

RESULTS

Streamflow Data

Historical mean annual flow for the Columbia during the historical (1916-1998) period was ~5,619 m^3/s (~198,433 ft^3/s). Estimated 10th percentile flow was ~4,072 m^3/s (143,801 ft^3/s), and estimated 90th percentile flow was 7,015 m^3/s (~247,732 ft^3/s). Notable (<10th percentile) single-year low flows occurred in 1926, 1929-1931, 1937, 1944, 1977, 1992, and 1994. Single-year high flows occurred in 1916, 1921, 1928, 1948, 1951, 1956, 1965, 1971-1972, 1974, 1976, 1982, and 1996-1997. Comparing the 1858-1915 portion of the historical record to the model-verified 1916-1998 10th and 90th percentiles, there are no additional years with flows lower than the 10th percentile, but 12 years (consecutive in 1879-1881) with high flows greater than the 90th percentile. This suggests either streamflows were frequently higher in the late 19th Century than the later historical average, or the stage height estimates (1858-1878) are biased high. We know of no evidence for the latter, and the channel cross section at The Dalles is basalt and therefore presumably very stable over time, so we take these observations as strong evidence the second half of the 19th Century frequently exhibited high flows in the Columbia River.

Tree-Ring Screening and Hydroclimatic Correlations

A total of 82 chronologies were significantly correlated ($p \leq 0.05$) with Columbia flow (34 negative, 27 positive, 7 negative lag 1, 14 positive lag 1) from 1916 to 1979 and were retained for further analysis (Figure 2, see Supporting Information). The retained chronologies used in the EOF/PC analysis or directly in regression-based reconstructions had moderate-to-strong correlations with climate variables related to streamflow (Supporting Information). The ten chronologies most negatively correlated (mean $r = -0.49$) with flow at The Dalles had their strongest correlations (all negative) with metrics of precipitation or snow: cool-season (Oct-Mar) precipitation, Mar-Jul SWE (r range $-$ 0.39 to -0.60), or in one case, summer precipitation (Table S1 in Supporting Information). The ten chronologies most positively correlated (mean $r = +0.40$) with flow had a mixed climate response. Their strongest correlations were with cool-season precipitation or May 1 SWE (four chronologies, r range +0.42 to +0.59) or, alternatively, warm-season (Apr-Sep or Jun-Aug) water balance deficit (six chronologies r range -0.34 to -0.62, Table S2 in Supporting Information).

For many of the chronologies with stronger flow correlations, both winter and summer responses were moderately strong, indicating either hydroclimatic limitation throughout the year or mechanisms linking cool- and warm-season hydroclimatology to growing season tree growth. Among the chronologies with lower absolute correlations to streamflow, correlations with climatic variables were also generally weaker though still significant.

Chronology-Based Streamflow Reconstruction: Calibration, Validation, and Verification

Five chronologies (three negatively correlated, two positively correlated) yielded the best calibration regression model (Table 1), with an $R^2 = 0.59$ and RE 0.50. The common period for all chronologies was 1609-1983, with minimum sample depth of 38 (chronology average 7.6) in 1609. The chronology-based reconstruction verification statistics (Table 1) indicate moderate-to-good performance of the calibration model over different portions of the calibration period and also the withheld flow data for 1858 to 1916.

To explore the limit of skillful reconstruction back in time, we developed a longer reconstruction back to 1502 (minimum sample depth of 43, chronology average 8.6) using the same methods, but limited to those chronologies extending prior to 1550. This resulted in a similar model, but the WA081 and Mt. Jefferson High were replaced by the OR087 (negative correlation with flow) and CANA220 (positive correlation with flow) chronologies. The calibration and validation for this reconstruction indicates a slight tradeoff in skill for the extra century of data coverage ($RMSE_v$ for 1609 reconstruction of 724 m^3/s compared to 802 m^3/s for the 1502 reconstruction) (Table 1). Both the 1609 and 1502 reconstructions were satisfactory for Durbin-Watson and VIF statistics (Table 1), although the split-sample verifications for the 1502 reconstruction do not perform as well as the 1602 reconstruction.

EOF/PC Analysis

Using the criterion from North *et al.* (1982) as modified by Bretherton *et al.* (1999) to account for

TABLE 1. Years 1609 and 1502 Chronology-Based Reconstruction Predictors, Parameter Estimates, and Diagnostics and Verification Statistics. See Supporting Information for Chronology Metadata and Species.

1609 Reconstruction Coefficients (species)	***r* (flow)**	**Estimate**	**Std. Error**	***t***	***p*(>|*t*|)**	**VIF**
Intercept		6,302.1	1,169	5.391	<0.0001	
CPL (LALY)	−0.411	−858.5	246.5	−3.483	0.0009	1.04
Mt Jefferson High (TSME)	−0.512	−1,267.7	371.6	−3.411	0.0011	1.27
wa081 (ABAM)	−0.466	−1,156.5	363.6	−3.18	0.0023	1.19
id010 (PIAL)	0.453	1,492.8	497.2	3.002	0.0039	1.28
or030 (PIPO)	0.395	1,112.5	378.4	2.94	0.0046	1.21
Model Diagnostics			**Verification**	**R^2 (adj)**	**RE**	**VIF**
Multiple $R^2 = 0.62$; Adj. $R^2 = 0.59$			1858-1915, withheld	0.42	0.32	1.08-1.60
$F = 20.23$ on 5 and 62 *DF*, $p < 0.0001$			1858-1982, every other year	0.46	0.38	1.03-1.14
RE = 0.50; RMSEv = 724 m^3/s			1859-1983, every other year	0.56	0.5	1.05-1.24
Durbin Watson = 2.23, $p = 0.7622$			1916-1949	0.56	0.44	1.25-1.86
			1950-1983	0.55	0.43	1.11-1.63
1502 Reconstruction Coefficients (species)	***r* (flow)**	**Estimate**	**Std. Error**	***t***	***p*(>|*t*|)**	**VIF**
Intercept		3,320.8	1,009.1	3.291	0.0016	
or030 (PIPO)	0.395	1,646.9	354	4.653	<0.0001	1.04
id010 (PIAL)	0.453	1,922.3	483.5	3.976	0.0002	1.14
CPL (LALY)	−0.411	−907.5	243.4	−3.728	0.0004	1.03
or087 (TSME)	−0.497	−1,018.1	465.5	−2.187	0.0321	1.21
cana220 (PIFL)	0.358	490.9	244.7	2.006	0.0488	1.08
Model Diagnostics			**Verification**	**R^2 (adj)**	**RE**	**VIF**
Multiple $R^2 = 0.55$; Adj. $R^2 = 0.52$			1858-1915, withheld	0.43	0.31	1.10-1.62
$F = 17.18$ on 5 and 69 *DF*, $p < 0.0001$			1858-1982, every other year	0.38	0.21	1.25-1.85
RE = 0.39; RMSEv = 802 m^3/s			1859-1983, every other year	0.42	0.32	1.10-1.33
Durbin Watson = 1.86, $p = 0.2152$			1916-1949	0.38	0.31	1.02-1.31
			1950-1983	0.63	0.50	1.05-1.27

sampling error and the effective change in degrees of freedom associated with temporal autocorrelation (Bretherton *et al.*, 1992), we estimated a range for each calculated EOF/PC eigenvalue and compared it with the range for neighboring eigenvalues. This allows more objective truncation of the EOF/PC spectrum and provides a hedge against using PC predictors that are in reality spurious. We considered the leading four (of 34) negative, two (of 27) positive, two (of 7) lag 1 negative, and two (of 14) lag 1 positive PCs to be independent and retained them for further analysis (Table 2). The leading positive PC (Figure 3) is a combined signal primarily from lower elevation chronologies (minimum sample depth 407, chronology mean 12.0) across the region (Figures 2 and 4), whereas the leading negative PC (Figure 3) is a combined signal from high-elevation chronologies (sample depth 414, chronology mean 15.3) in the Cascades and northern U.S. Rockies (Figures 2 and 4).

EOF/PC-Based Reconstruction: Calibration, Validation, and Verification

Using the principal components derived from the chronologies in a stepwise, forward selection multiple regression resulted in a calibration model (Table 3) based on the first and fourth PCs of negatively correlated chronologies, the first PC of positively correlated chronologies, the first PC of the lag 1 negative chronologies, and the second PC of the lag 1 positive chronologies.

The calibration model explained 48% of the variation in flow during the calibration period. The reduction in error statistic for the calibrated model was 0.41, indicating some model skill. The root mean square error of validation was 805 m^3/s (28,443 ft^3/s, or about 14% of historical mean flow). The calibration model satisfied assumptions of noncollinearity among predictors (VIF < 3), and a Durbin-Watson test for autocorrelation in the residuals was not significant, supporting an assumption of independence. The reconstruction developed from this model covers the common period of the EOF/PC analyses — 1637-1980.

The PC-based model verification results (Table 3) indicate acceptable model performance for different subsets of the calibration period. The verification period 1916-1947 had the weakest performance, whereas the 1948-1980 verification had the strongest, with the two every-other-year verification periods scoring in between.

Reconstruction Comparison

For both the 1609 and 1502 reconstructions the calibration and verification tests (Table 1) indicated that the chronology-based approach provided more skill than the PC-based reconstruction (Table 3). All three models fail to capture some extreme high- and low-flow years (Figure 5). The PC-based reconstruction best captured the high flows, with a mean error for 90th percentile and above of -516 m^3/s (1502: -845 m^3/s, 1609: -782 m^3/s). The 1609 reconstruction best captured the low flows, with a mean error for 10th percentile and below of $+668$ m^3/s (1502: $+800$ m^3/s, PC: $+1{,}075$ m^3/s). The sign of the single-year flow anomalies for all three reconstructions is generally correct when compared to the overlapping observed record: 77% for the 1502 reconstruction, 78% for the 1609 reconstruction, and 83% for the PC-based reconstruction.

Given the skill of the chronology-based reconstructions and the statistical superiority of the 1609 reconstruction, we chose to extend the length of the 1609 using methods equivalent to those used in Pederson *et al.* (2011) and Gray *et al.* (2011). Briefly, we adjusted the mean and variance of the 1502-1608 portion of the 1502 reconstruction to match that of the 1609 reconstruction (including error estimates, which increase with such rescaling), and then combined them to produce a record spanning 1502-1983 for use in further analyses (Figure 6).

Hydroclimatic Features of Reconstructed Streamflow

Here, we define extreme low- and high-flow events on the Columbia River as any event that has estimated

TABLE 2. EOF/PC Analyses, Common Period of Analysis, Retained PCs, and Correlation with Observed Flow.

EOF/PC Analysis of Correlated Chronologies	Common Period	PCs Retained (variance explained)	Correlation with Observed Flow
Negative *r*	1610-1980	1[1] (0.32), 2 (0.16), 3 (0.07), 4[1] (0.06)	1: −0.57[1]; 2: −0.07; 3: 0.02; 4: −0.13[1]
Positive *r*	1627-1980	1[1] (0.33), 2 (0.11)	1: 0.48[1]; 2: −0.17
Lag 1 Negative *r*	1637-1980	1[1] (0.38), 2 (18)	1: −0.10[1]; 2: 0.10
Lag 1 Positive *r*	1629-1980	1 (0.26), 2[1] (0.14)	1: 0.07; 2: 0.13[1]

[1]PCs retained and used in PC-based calibration model.

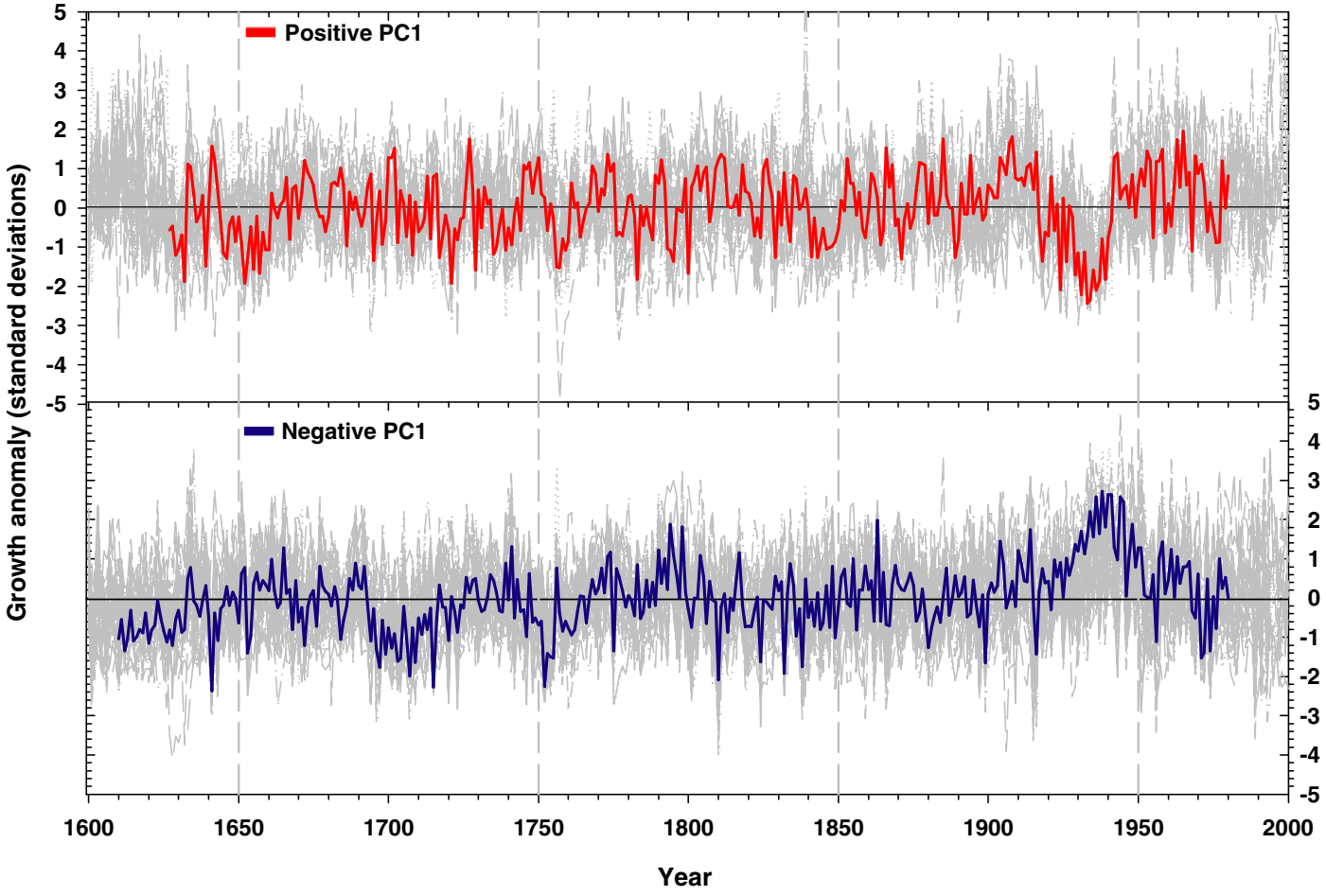

FIGURE 3. Leading Principal Components (PCs) from Chronologies Positively (above, 1627-1980) and Negatively (below, 1610-1980) Correlated with Historical Columbia Flow. Rescaled standard positively (n = 27) and negatively (n = 34) correlated chronologies used to compute the first PCs are shown in lighter background lines.

flow volumes lower (higher) than the 10th (90th) percentile of the hybrid reconstruction record (Figure 6). In total, the record yields 49 individual extreme low-flow years (≤10th percentile) and 41 individual high-flow events (≥90th percentile) (Table 4).

Noteworthy single-year extreme low-flow events of the 20th Century include 1930-1931, 1936, 1940-1941, 1944-1945, 1973, and 1977, and are only rivaled by single-year events in the early 1500s and during the droughts of the 1630s to 1650s (Figure 7). Individual year extreme high flows above the 90th percentile appear more frequently between the 1700s and 1800s (n = 28), with only seven events occurring during the 20th Century.

Although individual extreme events can pose challenges to water management, consecutive years, or "runs," of sustained high and low flows often prove the most challenging for water managers. In particular, the reconstructed multiyear flow volumes sustained below the 10th and 25th percentile, and above the 75th and 90th percentile as shown in Figure 7 may produce hydroclimatic conditions that affect either hydropower production or water supply (drought), or flood control (high flows). For example, the 1502-1513 drought is the only period of sustained low flow that rivals the 1929-1941 events in both severity and duration — both droughts had runs of 12 or more years below the 25th percentile and 4 years below the 10th percentile. The period 1929-1941 is continuously below the 15th reconstructed percentile and the 28th observed percentile (Figure 7). However, the 46-year period between 1622 and 1667 shows 80% of its water years with flow volumes below the 50th percentile and 48% below the 25th percentile. This period of sustained low flows also includes two runs of years below the 10th percentile (1633-1635 and 1651-1652). While this event (or two separate back-to-back events) is punctuated by a few above-average years, it appears to be a time of consistently low flows at approximately decadal time frames. In contrast, the period between the end of the 17th Century and the 1760s appears to have been a time of sustained and extreme high flows. This is particularly

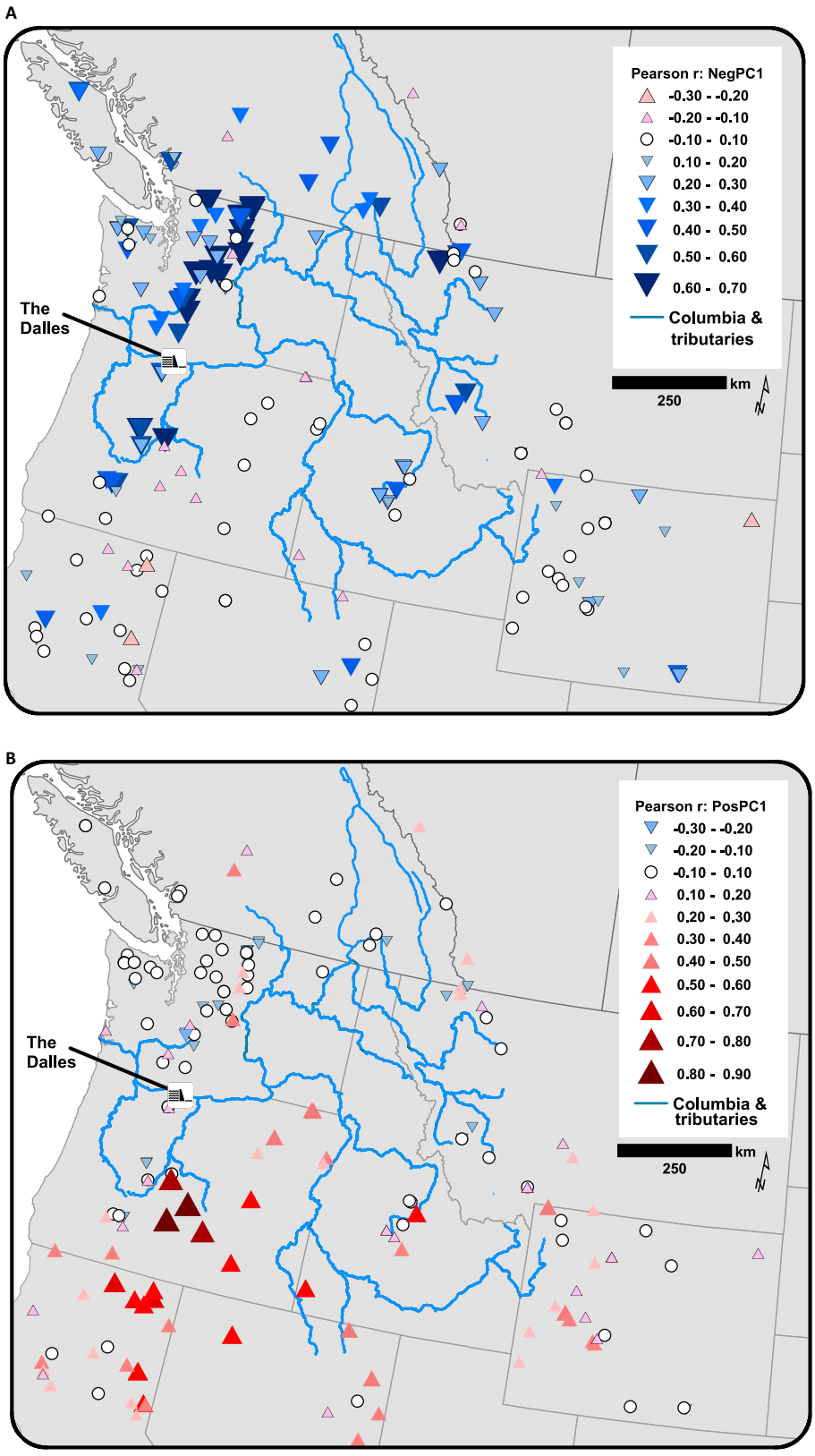

FIGURE 4. Maps of Correlations between Standard Chronologies and Leading Principal Components Retained for EOF/PC-Based Reconstruction. Top: negative PC1 composed mostly of high-elevation chronologies negatively correlated with winter precipitation. Bottom: positive PC1 composed mostly of low-elevation chronologies positively correlated with precipitation.

TABLE 3. Regression and Verification Table for PC-Based Calibration Model (1916-1980).

1637 Reconstruction Coefficients	**Estimate**	**Std. Error**	***t***	***p*(>|*t*|)**	**VIF**
(Intercept)	5,999.0	127.3	47.117	<0.0001	
Negative PC1	−504.8	115.1	−4.387	<0.0001	1.515
Positive PC1	401.8	126.2	3.183	0.0023	2.323
L1 Negative PC1	−676.6	263.7	−2.566	0.0129	1.382
Negative PC4	−652.9	259.2	−2.519	0.0145	1.233
L1 Positive PC2	−592.5	325.7	−1.819	0.0739	1.723

Model Diagnostics	**Verification**	**R^2 (adj)**	**RE**	**VIF**
Multiple R^2 = 0.52; Adj. R^2 = 0.48	1858 to 1980, every other year	0.40	0.3	1.38-1.85
F = 12.61 on 5 and 59 DF, $p < 0.0001$	1859 to 1979, every other year	0.37	0.29	1.25-1.44
RE = 0.41; RMSEv = 805 m^3/s	1916-1947	0.32	0.15	1.47-2.59
Durbin Watson = 2.04, p = 0.4689	1948-1980	0.47	0.31	1.29-1.62

true for the 39 years between 1696 and 1734 when only 2 years (1721 and 1723) had flows below the 50th percentile, and 69% of the years exceeded the reconstructed 75th percentile. Surprisingly, 41% of the years in this interval of high flows are estimated to have exceeded the extreme 90th percentile. The only 20th Century event that resembles such sustained high flows is the 31-year period between 1946 and 1976, when all but six years were above the 50th percentile, 45% of those exceeded the 75th percentile, and four exceeded the 90th percentile.

DISCUSSION

Reconstruction Methodological Considerations

The two reconstruction methods examined here resulted in proxy records that have numerous key features in common. In particular, both approaches indicated high streamflows in the early 1700s, mid-1700s, and early 1810s, and low streamflows during the early 1600s and 1930s. There are, however, important differences. For example, the PC-based reconstruction includes relatively high flows in the 1640s to 1660s, whereas the chronology-based reconstruction tends toward drought over this same period. This discrepancy may be due to low sample depth (i.e., number of trees in each chronology) in the early portions of some of chronologies retained for EOF/PC analysis. Sample size artifacts are minimized in both reconstructions by variance stabilization in chronology construction and in the chronology-based reconstruction because the underlying time series are composed of longer samples assembled from larger numbers of trees. The increased statistical skill of the chronology-based reconstruction over the PC-based reconstruction also suggests a dampening of important hydrologic signals as a result of the EOF/PC analysis itself. More specifically, in the EOF/PC approach, the signal may be diluted by giving equal weight to all significantly correlated chronologies, rather than filtering for only the strongest relationships as occurred in the development of the chronology-based reconstruction. Taken as a whole, this suggests the chronology-based reconstruction would be the most appropriate choice for applications in hydroclimatic analyses and water resource management.

It should also be noted both methods miss the magnitude of some observed extremes, and both reconstructions fail to capture near normal flow years (e.g., 1934, 1935, and 1938) in the midst of a relatively dry period from 1929-1941 (Figure 5). Flows in the 1930s as shown in the chronology-based reconstructed streamflow are about 260 m^3/s too high on average (roughly equivalent to the difference between the 25th and 30th percentile). The chronology-based reconstruction better captured low flows observed in 1944 and 1977, but both reconstructions underestimate the 1926 dry event. Because we did not rescale the variance of either reconstruction to match the observed record, reconstructed extremes are likely to be conservative (i.e., less extreme than actual). Future tree-ring-based reconstruction efforts might then focus on capturing extreme single-year events, while also using a variety of methods to explore the causes and consequences of uncertainty in historical records.

Comparison with Other Regional Hydroclimate Reconstructions

The composite 1502-1983 reconstruction is significantly correlated with the regional average of the

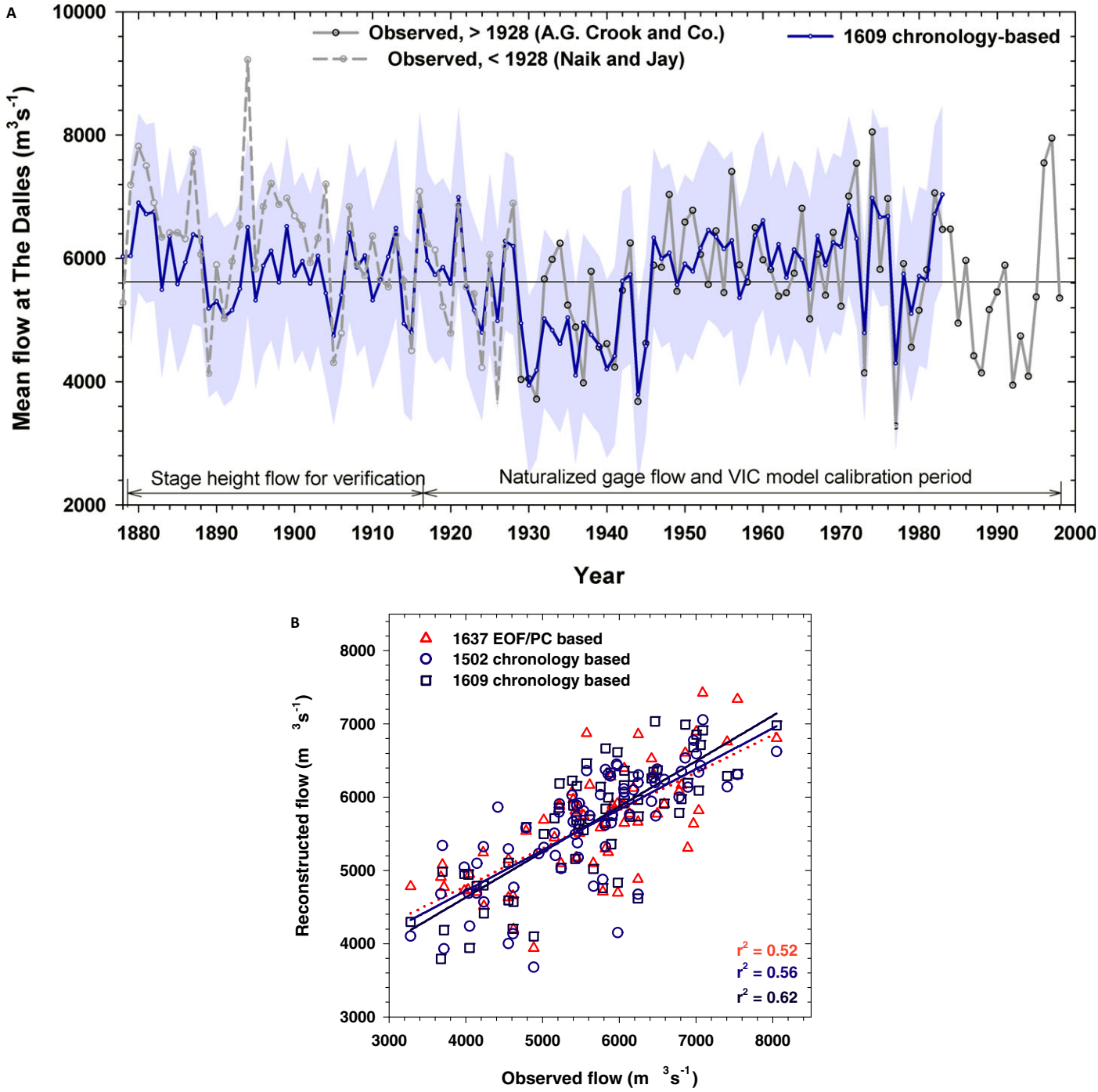

FIGURE 5. Calibration and Verification Period Flow for Best (1609) Reconstruction and Relationships for Each of the Streamflow Reconstruction Approaches. (A) Composite observed (1878-1928 stage height, 1928-1998 gage) naturalized Columbia River streamflow compared to 1609 chronology-based reconstructed streamflow with confidence intervals. (B) Calibration period relationships between observed and reconstructed streamflow for 1502, 1609, and PC-based reconstructions.

Cook *et al.* (2004) PDSI gridpoint reconstructions (which share some chronologies) for the Columbia Basin region at $r = 0.41$. The composite reconstruction presented here is weakly but significantly correlated with reconstructions of Snake River flow ($r = 0.33$ for 1591-1990 with Wise, 2010), Upper Yellowstone River flow ($r = 0.30$ for 1706-1977 with Graumlich *et al.*, 2003), Klamath River flow ($r = 0.24$ for 1507-1990 with Meko *et al.*, 2014), and Sacramento River flow ($r = 0.23$ for 1502-1977 with Meko *et al.*, 2001). Reconstructed PDSI for the PNW (Cook *et al.*, 2004) indicates a tendency toward dry years

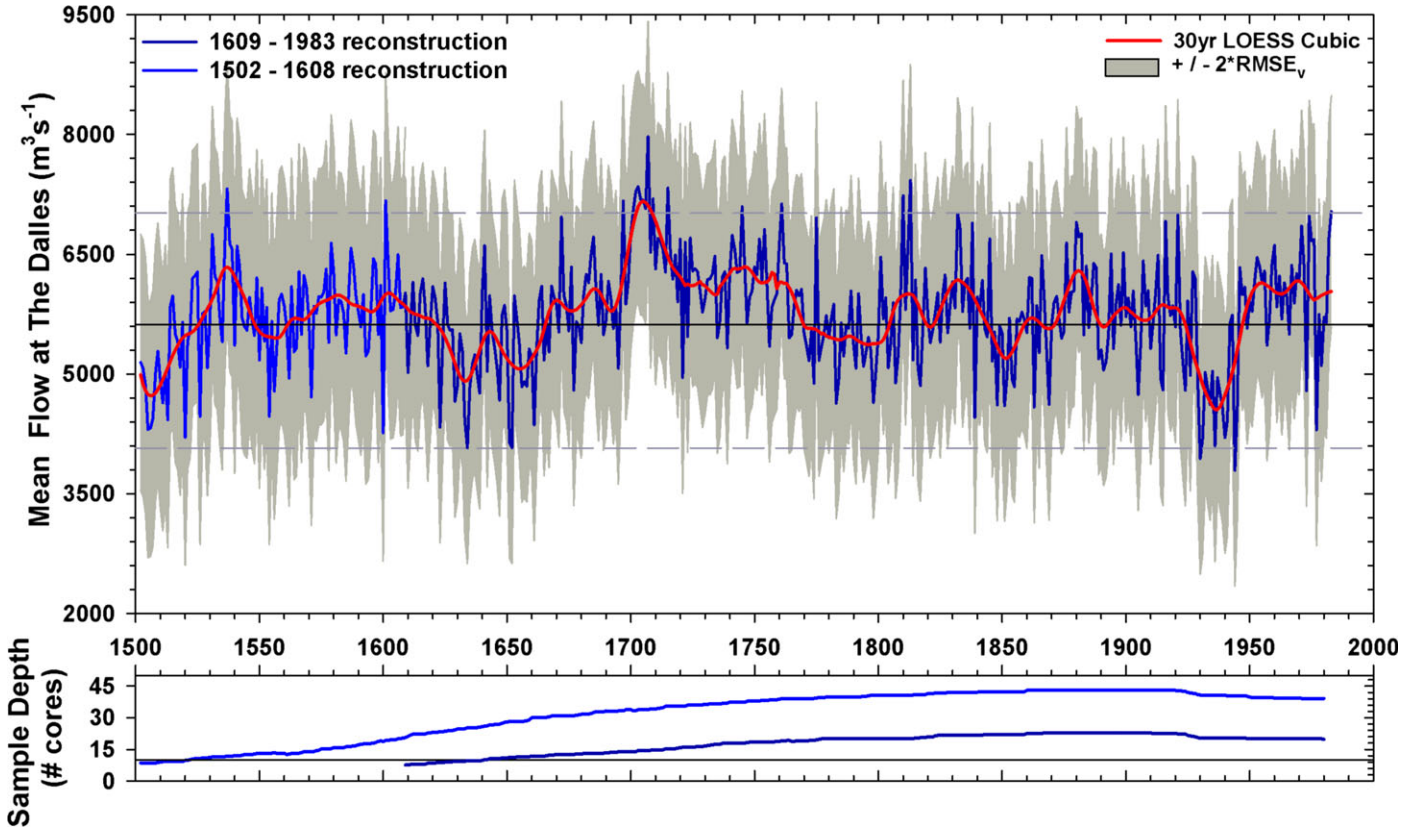

FIGURE 6. Composite Chronology-Based Reconstruction of Columbia River Flow at The Dalles, OR for 1502-1990 (top) and Sample Depth (mean cores per chronology, bottom). The estimated 10th and 90th percentile flows for the observed record are indicated by dashed lines, and the observed mean is shown as a solid line. Reconstruction 5th and 95th confidence intervals are estimated as two times the $RMSE_v$ (Meko *et al.*, 2001) and are shown as light gray background shading. Line in lower panel indicates sample depth of 10 cores/chronology.

TABLE 4. High (≥90th percentile) and Low (≤10th percentile) Reconstructed Columbia River Flows by Century.

	Century	Years
Years above 90th percentile reconstructed flows	1500s	1531, 1537
	1600s	1601, 1672, 1685, 1697
	1700s	1700-1707, 1709, 1711, 1715, 1720, 1724, 1741, 1745, 1752, 1754, 1761, 1775
	1800s	1810, 1813, 1832-1833, 1838, 1845, 1880-1882
	1900s	1916, 1921, 1971, 1974, 1976, 1982-1983
Years below 10th percentile reconstructed flows	1500s	1504-1507, 1511, 1513, 1520, 1526, 1554, 1556, 1571
	1600s	1600, 1623, 1629, 1633-1635, 1639, 1647, 1651-1652, 1656, 1658, 1661, 1677
	1700s	1783, 1798
	1800s	1839, 1848, 1851, 1855, 1863, 1869
	1900s	1905, 1915, 1924, 1930, 1931, 1933-1934, 1936, 1938-1941, 1944-1945, 1973

for the 1460s-1470s, 1630s-1640s, 1830s-1840s, and 1920s-1930s, although the 1920s-1930s appear drier than the 1460s-1470s and 1630s-1640s, which in turn are drier than the 1840s (see Figure 8). Reconstructions of PDSI and annual precipitation from central OR indicate the 1840s and 1920s and 1930s were likely periods of low annual precipitation (Garfin and Hughes, 1996; Knapp *et al.*, 2004) in this subregion of the Columbia Basin. Graumlich (1987) reconstructed annual precipitation in the "Western lowlands" (western Washington [WA] and northwestern OR), "Columbia Basin" (eastern WA and northeastern OR), and "Southern valleys" (southern OR and northeastern California) and found differences in the duration and magnitude of these events within the subregions. Particularly in the Western lowlands and Columbia Basin, multiyear droughts apparently occurred in the 1840s, and the early 20th Century drought appears strongest in the Southern Valleys but is evident in all three regions. The 1720s appear similar in magnitude, if not necessarily duration, in all three subregional reconstructions (Graumlich,

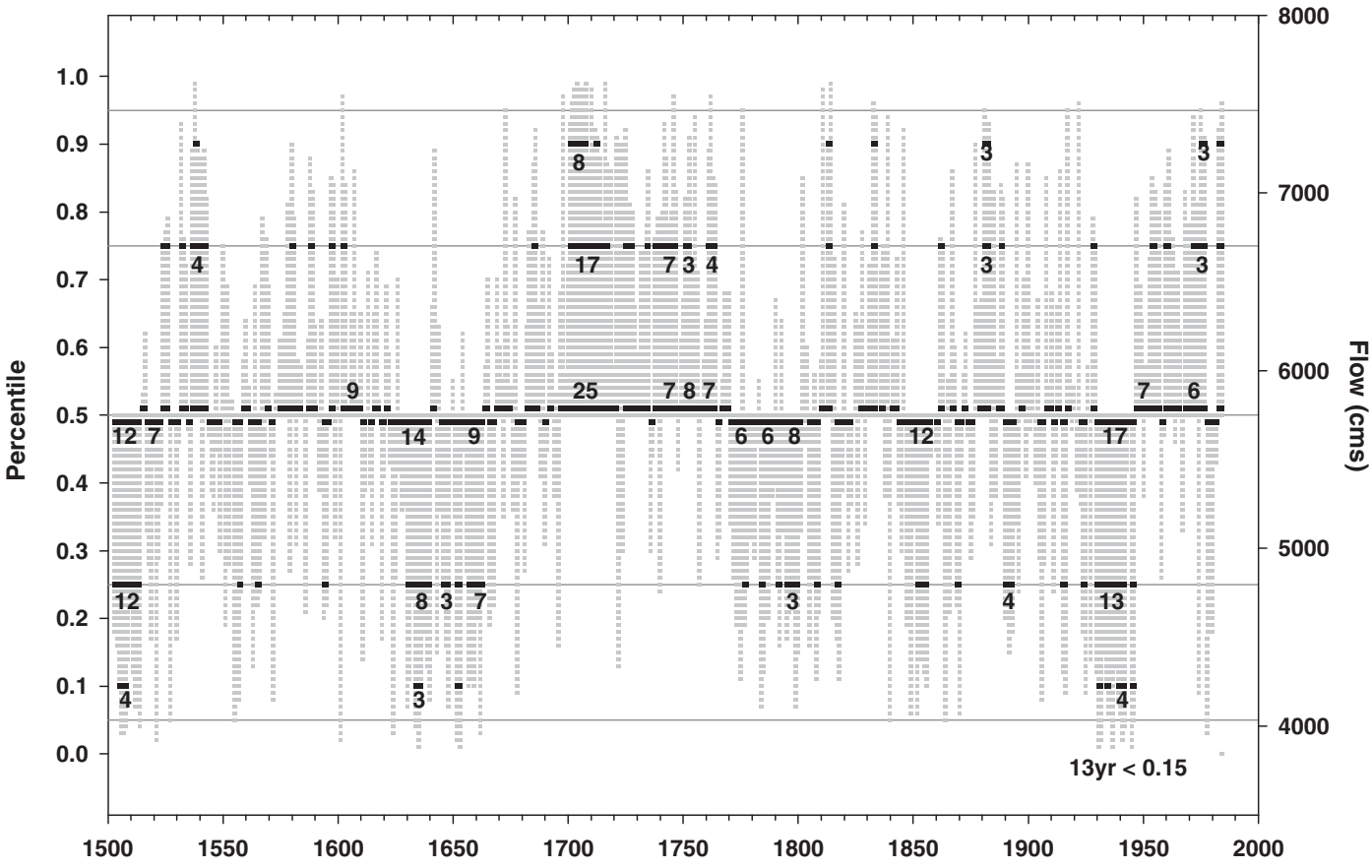

FIGURE 7. Reconstructed Flow Percentiles (left axis) and Magnitude (right axis) for Columbia Streamflow Reconstruction. Consecutive years with reconstructed annual flow below or above reconstructed percentile flows are indicated. Highlighted in black are selected percentiles below (gray lines indicate 5th, 25th, 49th) and above (gray lines indicate 51st, 75th, 95th) median flow. Runs (>5 year consecutive) above or below the 49th and 51st percentile and runs (>2 year consecutive) above/below the 10th/90th and 25th/75th percentiles are labeled with the duration of the run.

1987). In the Sacramento Basin for the years between about 1835 and the late 1840s, reconstructed flows are comparable to those in the early 1920s to the late 1930s (Meko *et al.*, 2001). Upper Klamath River water-year precipitation comparable in anomaly magnitude to the low flows of the 1910s to 1930s occurred in the mid-1600s (Figure 8) and the 1100s (Meko *et al.*, 2014).

Our reconstruction is consistent with previous work that identified periods of below-average moisture availability or streamflow in the 1620s-1630s, 1650s, 1840s, and 1930s (Figure 8; Graumlich, 1987; Cook *et al.*, 2004; Gedalof *et al.*, 2004; Wise, 2010; Malevich *et al.*, 2013; Meko *et al.*, 2014) and also indicates a period of low flows in the early 1500s. We did not identify low flow periods in the 1840s of the magnitude indicated by the Gedalof *et al.* (2004) reconstruction of Columbia River flow. The 1839, 1848, and 1851 reconstructed flows are all near the 20th percentile observed flow, and the period 1846-1852 is below the reconstruction and observed means, with mean flows around the 30th percentile observed. In contrast, the period 1929-1941, where all years in the reconstruction are below the observed mean, has six years below the 20th percentile (1930, 1931, 1936, and 1939-1941) and a mean around the 20th percentile. Between 1626 and 1639, all reconstructed flows are below the observed mean flow and mean flow was about the 27th percentile. This drought corresponds temporally with the drought identified by Wise (2010) for the Snake River, but our results suggest this event in the whole Columbia River Basin may have been of equal duration (longer if the 1640s are considered), but not necessarily more severe than the sustained low flows reconstructed for the period 1929-1941 given the uncertainty in the reconstructions. Our reconstruction also suggests a similar event about 1654-1662, with nine consecutive years of below-average flows and a mean flow around the 27th percentile. The reconstructed mean flow from 1502 to 1513 was lower, at about the 23rd percentile. We observed shorter and less severe low-flow periods in the 1770s, 1790s, and 1890s.

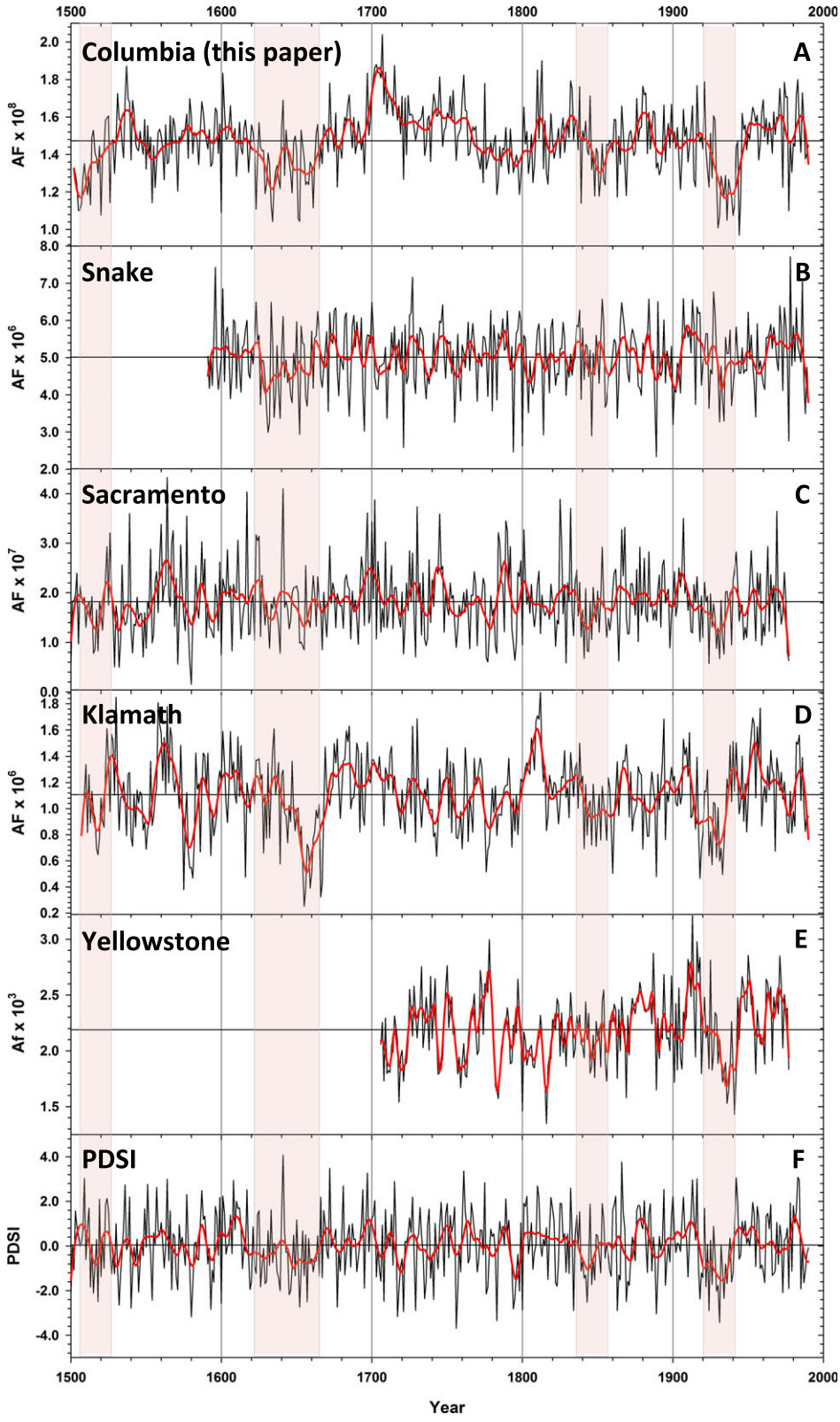

FIGURE 8. Comparison of Regional Hydroclimatic Reconstructions. Columbia River at The Dalles reconstruction (A, this study); Snake River at Heise (B, Wise, 2010); Sacramento River (C, Meko *et al.*, 2001); Klamath River (D, Meko *et al.*, 2014); Yellowstone River (E, Graumlich *et al.*, 2003); Palmer Drought Severity Index (PDSI) (F, Cook *et al.*, 2004, mean of 24 gridpoints covering the Columbia Basin). Red lines indicate 21-year LOESS smoothing, shaded bars highlight time periods discussed in the text.

One explanation of the lower severity of events in our reconstruction compared to other work is previous efforts did not explicitly incorporate chronologies that are strongly and directly linked to winter precipitation. In short, winter precipitation that can "make or break" a runoff year will likely be missed or muted when, as has often been the case, trees whose growth is more closely tied to summer soil moisture content form the foundation of the reconstruction. Another explanation is the reconstructions in general have moderate skill, so mismatches in timing (in this and/or other reconstructions) could be explained by reconstruction error alone. Finally, it is possible the temporal and spatial variation in drought timing over a geographical area this large is not an artifact of proxy selection and methodology, but represents real variation.

The Role of Seasonal Drought in Governing Flows on the Columbia

One key feature of the reconstructed Columbia flow record is droughts in the proxy record do not exceed the duration and magnitude of observed events. If anything, the low flows of the 1500s-1510s, 1620s-1630s, 1840s, and 1930s are roughly comparable in either duration or magnitude or both. Sustained high-flow periods in the 17th to 19th Centuries are, on the other hand, noticeably outside the bounds of the observed record (Figure 7). The chronology-based reconstruction suggests the 25 years between 1696 and 1720 were all above the mean observed flow, and 1700-1707 were consecutively above the 90th percentile of observed flow (mean 93rd percentile), which is unmatched in the rest of the proxy record. Other notable periods with runs of several years above mean observed flow apparently occurred from 1724-1734 (72nd percentile), 1740-1755 (76th percentile), 1757-1763 (76th percentile), 1809-1813 (83rd percentile), 1829-1836 (72nd percentile), and 1876-1882 (76th percentile). Except for 1957 and 1966, the entire period between 1950 and 1972 was above mean observed flow as well, with three runs of consecutive years between the 70th and 76th percentiles. The period of higher flows in the stage height portion of the observed streamflow record (from 1858-1877) is captured in the reconstructions presented here, as well as in the PDSI reconstruction and the Yellowstone River reconstruction, but not in some of the other hydroclimatic reconstructions. However, it is worth noting all the reconstructions underestimate high flows in the calibration period, indicating some loss of skill at the high end of the observed distribution.

The leading PC modes (Figure 3) indicate that the very high-flow period in the early 18th Century was related to high cool-season precipitation as there was a coherent period of sustained low growth among high elevation, snow-limited trees, and near-average growth among low elevation, summer water-limited trees. The snowpack reconstruction records from Pederson *et al.* (2011) also indicate this was a time of high snowpack in the U.S. Northern Rockies. Although it must be noted that the two reconstructions share some tree-ring data in common, the Northern Rockies 1 April SWE reconstruction (Pederson *et al.*, 2011) is moderately correlated with the Columbia composite reconstruction ($r = 0.50$) and well correlated with the PC representing cool-season precipitation in the EOF/PC reconstruction ($r = -0.70$).

During the reconstructed 1840s drought, the high-elevation, snowpack-limited trees appear to have been near normal growth, with below-average growth apparent in the low-elevation summer water-limited trees. This suggests potentially low flows of the 1840s were affected by warm-season drought, but offset to some extent by normal snowpack (or delayed melt of snowpack). This may also explain why other streamflow reconstructions driven more by antecedent soil moisture or otherwise water-limited chronologies identified the 1840s as a more severe low-flow event. The same may be true for the reconstructed low flows of the 1620s and 1630s as reconstructions of PDSI (Cook *et al.*, 2004) and drought-driven flows on the Snake River (Wise, 2010) highlight this period as low precipitation (Figure 8), but the leading PC of cool-season precipitation-sensitive chronologies indicates higher than normal snowpack. Standing in stark contrast to these events, the severe 1930s-1940s "Dust-bowl" droughts appear characterized by both low snowpack (low cool-season precipitation) and high warm-season water demand. In summary, seasonally sensitive tree-ring moisture records indicate the lowest flows in the Columbia River Basin occur when there are simultaneous low cool-season precipitation and either low warm-season precipitation or high warm-season water demand, but sustained (decadal) periods of below-average flow may occur in response to either seasonal mechanism.

Management Implications: Comparing Reconstructed and Potential Future Streamflow

The observed record (1916-1998) clearly underestimates the possibility of the sustained high flows evident in reconstructed streamflow and in the late 19th Century streamflow observations, and the annual and decadal low flows observed during this period are comparable in severity to those in the reconstructions, but there is evidence of longer droughts.

Decadal droughts of similar magnitude and duration to those observed in the early 20th Century have occurred before, and the period in the early to mid-1600s may have been a period with sustained low flows for most of several decades. The frequency of such events cannot be estimated conclusively given the length of these reconstructions.

Interpreting the reconstructions presented here only in the context of historical discharge is perhaps insufficient to understand the full implications for the Columbia water resources decision context. Future annual streamflow in the Columbia depends both on the interannual to multidecadal variability in precipitation and the influence of global climate forcing on regional trends in precipitation and temperature. Global climate model (GCM) precipitation projections for the PNW suggest a modest (+1%-+2%) increase in annual precipitation averaged across 39 GCM/emission scenarios combinations, although many models suggest an increase in winter precipitation and decrease in summer precipitation (Mote and Salathé, 2010). From these scenarios, Elsner *et al.* (2010) developed statistically downscaled climate forcings for the Columbia River Basin and used them to drive the VIC hydrologic model (Elsner *et al.*, 2010). In a second study using a calibrated version of the same hydrologic model, the Hybrid Delta (HD) downscaling approach was used to develop 10 scenarios of future streamflow in the Columbia River (10 GCMs run under SRES A1B, Hamlet *et al.*, 2013; Tohver *et al.*, 2014). These scenarios indicate that the timing of peak and low flows could be expected to change considerably. However, despite increased evaporation, the total annual flow increased in response to winter precipitation increases (Elsner *et al.*, 2010). We used the 2030-2059 A1B projected streamflows for 10 GCMs in Hamlet *et al.* (2013) to develop quantile distributions for future streamflow at The Dalles. These scenarios are reasonable because CMIP3 and CMIP5 generations of GCMs can be considered as from the same probability distribution of realizations (Knutti and Sedlacek, 2013) and because differences among emissions scenarios during this midcentury period are small compared to end of century. Comparing these projections to quantile distributions of the observed, naturalized, and reconstructed flows presented here (Figure 9), the observed and most GCM-projected flows have lower flow for a given probability below about the 20th percentile than the tree-ring reconstructed flow record (Figures 6 and 9). The same is true, and of greater magnitude, for high annual flows. If the errors in quantiles of the reconstructed flows are comparable to the uncertainty in the GCM projections, this indicates a larger future range of hydrologic variability despite a much higher number of realizations in the reconstructed record.

Notable differences arise in the lower and particularly upper quartile of reconstructed *vs.* future flows (Figure 9), for which the future extremes could exceed events indicated in the observed and reconstructed flow records. The potential sequence of events in future flows on time scales of more than a year or two,

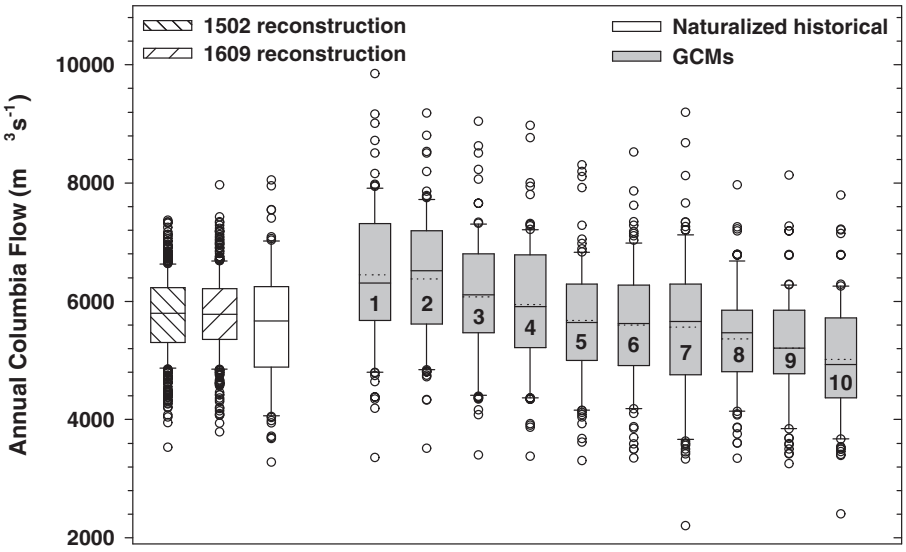

FIGURE 9. Quantile Distributions for 1502 and 1609 Reconstructions, Naturalized Historical Flows, and Future (2030-2059) A1B Global Climate Model (GCM) Scenarios. GCM projections (1-10) are derived from downscaling that preserves the historical annual sequences. Therefore, the range of future streamflows is from a distribution that includes the observed interannual and decadal variability, but they do not allow for novel sequences of interannual to decadal variability. GCMs: 1-MIROC 3.2; 2-CGCM 3.1 t47; 3-IPSL cm4; 4-HADCM; 5-CNRM cm3; 6-ECHAM 5; 7-CCSM 3; 8-ECHO-G; 9-PCM 1; 10-HADGEM 1.

however, may be more important challenges for water resources management than whether a single year is at the upper or lower extreme of flows.

Future hydroclimate simulations indicate the potential for changes in extreme years, and GCMs suggest larger increases in high-flow years than decreases in low annual flows. All the GCMs, however, project climate that would lead to lower annual flows in some years than any observed in either of the chronology-based reconstructions. The projected future quantile distribution range from ten plausible GCM scenarios is even greater than the reconstructed distribution of flows over the past 500 years, so resource planning based on these scenarios may be sufficient in terms of probable magnitude of annual flow volumes, but the time series of the downscaled GCM results is based on history from 1916-2006 and the reconstructions may provide more realistic scenarios of decadal runs and flow sequences assuming the persistence in the reconstructions from the standard chronologies is realistic. The atmospheric and ocean conditions that lead to the physical responses resulting in the reconstructed events (both high and low annual flows and, in particular, the decade long runs of high or low years) are yet unknown, so the combination of climate change and natural variability cannot be conclusively estimated as the downscaled GCM scenarios summarized here use variability consistent with the 20th Century variability observed in the region Mantua *et al.* (1997). Although beyond the scope of this study, the approaches developed by Lutz *et al.* (2012), Ault *et al.* (2014), or Cook *et al.* (2015), could be used in conjunction with this streamflow reconstruction to better assess future drought and/or flood risk by combining information from the paleoproxy record with changes in the probability distributions from GCM projections. This would provide a more explicit and detailed understanding of the combined effects of natural low-frequency climate variability with future anthropogenically driven changes to climate.

SUPPORTING INFORMATION

Additional supporting information may be found online under the Supporting Information tab for this article: Chronologies used in reconstructions.

ACKNOWLEDGMENTS

This study was partially funded through NOAA CPO SARP (NA07OAR4310371, N. Mantua, J. Littell, and A. Hamlet). This publication was partially funded by the University of Washington Climate Impacts Group and the Department of Interior Alaska Climate Science Center. We thank Contributors of the International Tree-Ring Data Bank, IGBP PAGES/World Data Center for Paleoclimatology, NOAA/NCDC Paleoclimatology Program, Boulder, Colorado, USA. Andrew Bunn evaluated code for estimating EOF/PC degrees of freedom. We thank Greg McCabe, Jeff Lukas, and two anonymous reviewers for helpful comments on previous versions of the manuscript. Any use of trade, firm, or product names is for descriptive purposes only and does not imply endorsement by the U.S. Government.

LITERATURE CITED

A.G. Crook Company, 1993. Adjusted Streamflow and Storage: Columbia River and Coastal Basins, 1928 -1989. Prepared for Bonneville Power Administration, Contract No. DE-AC79-92BP21958.

Allen, D.M., 1971. The Prediction Sum of Squares as a Criterion for Selecting Predictor Variables. Technical Report Number 23, Department of Statistics, University of Kentucky.

Ault, T.R., J.E. Cole, J.T. Overpeck, G.T. Pederson, and D.M. Meko, 2014. Assessing the Risk of Persistent Drought Using Climate Model Simulations and Paleoclimate Data. Journal of Climate 27:7529-7549.

Ault, T.R., J.E. Cole, J.T. Overpeck, G.T. Pederson, S. St George, B. Otto-Bliesner, C.A. Woodhouse, and C. Deser, 2013. The Continuum of Hydroclimate Variability in Western North America During the Last Millennium. Journal of Climate 26:5863-5878.

Bonneville Power Administration, Bureau of Reclamation and U.S. Army Corps of Engineers, 1995. Columbia River System Operation Review: Final Environmental Impact Statement. U.S. Department of Energy Report No. DOEJEIS-0170.

Bretherton, C.S., C. Smith, and J.M. Wallace, 1992. An Intercomparison of Methods for Finding Coupled Patterns in Climate Data. Journal of Climate 5:541-560.

Bretherton, C.S., M. Widmann, V.P. Dymnikov, J.M. Wallace, and I. Bladé, 1999. The Effective Number of Spatial Degrees of Freedom of a Time-Varying Field. Journal of Climate 12:1990-2009.

Briffa, K.R., 1995. Interpreting High-Resolution Proxy Climate Data—The Example of Dendroclimatology. *In*: Analysis of Climate Variability: Applications of Statistical Techniques, H. von Storch and A. Navarra (Editors). Springer Verlag, Berlin, pp. 77-94.

Bumbaco, K.A. and P.W. Mote, 2010. Three Recent Flavors of Drought in the Pacific Northwest. Journal of Applied Meteorology and Climatology 49:2058-2068.

Cook, B.I., T.R. Ault, and J.E. Smerdon, 2015. Unprecedented 21st Century Drought Risk in the American Southwest and Central Plains. Science Advances 1:e1400082.

Cook, E.R., 1985. A Time Series Analysis Approach to Tree-Ring Standardization. Ph.D. Dissertation, University of Arizona, Tucson, Arizona.

Cook, E.R. and R.L. Holmes, 1999. Program ARSTAN User's Manual. Laboratory of Tree-Ring Research, University of Arizona, Tucson, Arizona.

Cook, E.R. and G.C. Jacoby, 1983. Potomac River Streamflow Since 1730 as Reconstructed by Tree Rings. Journal of Applied Meteorology 22:1659-1672.

Cook, E.R., C. Woodhouse, C.M. Eakin, D.M. Meko, and D.W. Stahle, 2004. Long-Term Aridity Changes in the Western United States. Science 306:1015-1018.

Daly, C., M. Halbleib, J.I. Smith, W.P. Gibson, M.K. Doggett, G.H. Taylor, J. Curtis, and P.A. Pasteris, 2008. Physiographically-Sensitive Mapping of Temperature and Precipitation across the

Conterminous United States. International Journal of Climatology 28:2031-2064.

Daly, C., R.P. Neilson, and D.L. Phillips, 1994. A Statistical-Topographic Model for Mapping Climatological Precipitation over Mountainous Terrain. Journal of Applied Meteorology 33:140-158.

Elsner, M.M., L. Cuo, N. Voisin, J.S. Deems, A.F. Hamlet, J.A. Vano, K.E.B. Mickelson, S.Y. Lee, and D.P. Lettenmaier, 2010. Implications of 21st Century Climate Change for the Hydrology of Washington State. Climatic Change 102:225-260.

Fritts, H.C., 1976. Tree Rings and Climate. The Blackburn Press, Caldwell, New Jersey, ISBN: 1-930665-39-3.

Garfin, G.M. and M.K. Hughes, 1996. Eastern Oregon Divisional Precipitation and Palmer Drought Severity Index from Tree-Rings. Report to the U.S. Forest Service Intermountain Research Station. USDA Forest Service Cooperative Agreement PNW 90-174.

Gedalof, Z., D.L. Peterson, and N.J. Mantua, 2004. Columbia River Flow and Drought Since 1750. Journal of the American Water Resources Association 40:1579-1592.

Gedalof, Z. and D.J. Smith, 2001. Dendroclimatic Response of Mountain Hemlock (Tsuga mertensiana) in Pacific North America. Canadian Journal of Forest Research 31:322-332.

Graumlich, L.J., 1987. Precipitation Variation in the Pacific Northwest (1675-1975) as Reconstructed from Tree Rings. Annals of the Association of American Geographers 77:19-29.

Graumlich, L.J., M.F.J. Pisaric, L.A. Waggoner, J.S. Littell, and J.C. King, 2003. Upper Yellowstone River Flow and Teleconnections with Pacific Basin Climate Variability During the Past Three Centuries. Climatic Change 59:245-262.

Gray, S.T., J.J. Lukas, and C.A. Woodhouse, 2011. Millennial-Length Records of Streamflow from Three Major Upper Colorado River Tributaries. Journal of the American Water Resources Association 47:704-712.

Gray, S.T. and G.J. McCabe, 2010. A Combined Water Balance and Tree-Ring Approach to Understanding the Potential Hydrologic Effects of Climate Change in the Central Rocky Mountain Region. Water Resources Research 46:W05513, DOI: 10.1029/2008WR007650.

Hamlet, A.F., M.M. Elsner, G. Mauger, S.Y. Lee, and I. Tohver, 2013. An Overview of the Columbia Basin Climate Change Scenarios Project: Approach, Methods, and Summary of Key Results. Atmosphere-Ocean 1:392-415.

Hamlet, A.F. and D.P. Lettenmaier, 2005. Production of Temporally Consistent Gridded Precipitation and Temperature Fields for the Continental U.S. Journal of Hydrometeorology 6(3): 330-336.

Hamlet, A.F., P.W. Mote, M.P. Clark, and D.P. Lettenmaier, 2005. Effects of Temperature and Precipitation Variability on Snowpack Trends in the Western U.S. Journal of Climate 18:4545-4561.

Hamlet, A.F., P.W. Mote, M.P. Clark, and D.P. Lettenmaier, 2007. Twentieth-Century Trends in Runoff, Evapotranspiration, and Soil Moisture in the Western U.S. Journal of Climate 20:1468-1486.

Hidalgo, H.G., T. Das, M. Dettinger, D.R. Cayan, D. Pierce, T. Barnett, G. Bala, A. Mirin, A.W. Wood, C. Bonfils, B.D. Santer, and T. Nozawa, 2009. Detection and Attribution of Streamflow Timing Change in the Western United States. Journal of Climate 22:3838-3855.

Hidalgo, H.G., T.C. Piechota, and J.A. Dracup, 2000. Alternative Principal Components Regression Procedures for Dendrohydrologic Reconstructions. Water Resources Research 36:3241-3249.

Holmes, R.L., 1999. User's Manual for Program COFECHA. Laboratory of Tree-Ring Research, University of Arizona, Tucson, Arizona.

Jain, S., C.A. Woodhouse, and M.P. Hoerling, 2002. Multidecadal Streamflow Regimes in the Interior Western United States: Implications for the Vulnerability of Water Resources. Geophysical Research Letters 29:2036-2039.

Knapp, P.A., P.T. Soulé, and H.D. Grissino-Mayer, 2004. Occurrence of Sustained Droughts in the Interior Pacific Northwest (A.D. 1733-1980) Inferred from Tree-Ring Data. Journal of Climate 17:140-150.

Knutti, R. and J. Sedlacek, 2013. Robustness and Uncertainties in the New CMIP5 Climate Model Projections. Nature Climate Change 3:369-373.

Lee, K.N., 1993. Compass and Gyroscope: Integrating Science and Politics for the Environment. Island Press, Washington, DC.

Littell, J.S., M.M. Elsner, G.S. Mauger, E.R. Lutz, A.F. Hamlet, and E.P. Salathé, 2011. Regional Climate and Hydrologic Change in the Northern U.S. Rockies and Pacific Northwest: Internally Consistent Projections of Future Climate for Resource Management. Project report for USFS JVA 09-JV-11015600-039. Prepared by the Climate Impacts Group, University of Washington, Seattle. April, 2011. http://cses.washington.edu/picea/USFS/pub/Littell_etal_2010/Littell_etal._2011_Regional_Climatic_And_Hydrologic_Change_USFS_USFWS_JVA_17Apr11.pdf, *accessed* March 2015.

Littell, J.S., D.L. Peterson, and M. Tjoelker, 2008. Douglas-fir Growth in Mountain Ecosystems: Water Limits Tree Growth from Stand to Region. Ecological Monographs 78:349-368.

Lutz, E.R., A.F. Hamlet, and J.S. Littell, 2012. Paleoreconstruction of Cool Season Precipitation and Warm Season Streamflow in the Pacific Northwest with Applications to Climate Change Assessments. Water Resources Research 48:W01525, DOI: 10.1029/2011WR010687.

Malevich, S.B., C.A. Woodhouse, and D.M. Meko, 2013. Tree-Ring Reconstructed Hydroclimate of the Upper Klamath Basin. Journal of Hydrology 495:13-22.

Mantua, N.J., S.R. Hare, Y. Zhang, J.M. Wallace, and R.C. Francis, 1997. A Pacific Interdecadal Climate Oscillation with Impacts on Salmon Production. Bulletin of the American Meteorological Society 78:1069-1079.

Maurer, E.P., D.P. Lettenmaier, and N.J. Mantua, 2004. Variability and Predictability of North American Runoff. Water Resources Research 40:W09306, DOI: 10.1029/2003WR002789.

Meko, D.M., C.W. Stockton, and W.R. Boggess, 1995. The Tree-Ring Record of Severe Sustained Drought. Water Resources Bulletin 31:789-801.

Meko, D.M., M.D. Therrell, C.H. Baisan, and M.K. Hughes, 2001. Sacramento River Flow Reconstructed to A.D. 869 from Tree Rings. Journal of the American Water Resources Association 37:1029-1040.

Meko, D.M., C.A. Woodhouse, C.H. Baisan, T. Knight, J.J. Lukas, M.K. Hughes, and M.W. Salzer, 2007. Medieval Drought in the Upper Colorado River Basin. Geophysical Research Letters 34 (10):L10705, DOI: 10.1029/2007GL029988.

Meko, D.M., C.A. Woodhouse, and R. Touchan. 2014. Klamath/San Joaquin/Sacramento Hydroclimatic Reconstructions from Tree Rings. Draft Final Report to California Department of Water Resources Agreement 4600008850. http://www.water.ca.gov/waterconditions/docs/tree_ring_report_for_web.pdf, *accessed* March 2015.

Menne, M.J., C.N. Williams, and R.S. Vose, 2009. The United States Historical Climatology Network Monthly Temperature Data - Version 2. Bulletin of the American Meteorological Society 90:993-1107.

Miles, E.M., A.K. Snover, A.F. Hamlet, B. Callahan, and D. Fluharty, 2000. Pacific Northwest Regional Assessment: The Impacts of Climate Variability and Climate Change on the Water Resources of the Columbia River Basin. Journal of the American Water Resources Association 36:399-420.

Mote, P.W. and E.P. Salathé, Jr., 2010. Future Climate in the Pacific Northwest. Climatic Change 102(1-2):29-50.

Naik, P.K. and D.A. Jay, 2005. Estimation of Columbia River Virgin Flow: 1879 to 1928. Hydrological Processes 19:1807-1824.

Neter, J., M.H. Kutner, C.J. Nachtsheim, and W. Wasserman, 1996. Applied Linear Statistical Models (Fourth Edition). McGraw-Hill/Richard D. Irwin, Chicago, ISBN-13: 978-0256117363.

North, G.R., T.L. Bell, R.F. Cahalan, and F.J. Moeng, 1982. Sampling Errors in the Estimation of Empirical Orthogonal Functions. Monthly Weather Review 110:699-706.

NRC, 1996. Upstream: Salmon and Society in the Pacific Northwest. National Academies Press, Washington, DC.

Pederson, G.T., S.T. Gray, C.A. Woodhouse, J.L. Betancourt, D.B. Fagre, J.S. Littell, E. Watson, B.H. Luckman, and L.J. Graumlich, 2011. The Unusual Nature of Recent Snowpack Declines in the North American Cordillera. Science 333:332-335.

Peterson, D.W. and D.L. Peterson, 2001. Mountain Hemlock Growth Responds to Climatic Variability at Annual and Decadal Scales. Ecology 82:3330-3345.

Preisendorfer, R.W., 1988. Principal Component Analysis in Meteorology and Oceanography, Developments in Atmospheric Sciences, Vol. 17. Elsevier, Amsterdam. ISBN: 13:978-0444430144.

Rice, J.L., C.A. Woodhouse, and J.J. Lukas, 2009. Science and Decision-Making: Water Management and Tree-Ring Data in the Western United States. Journal of the American Water Resources Association 45:1248-1259.

Robertson, C.S., 2011. Dendroclimatology of Yellow Cedar (*Callitropsis nootkatensis*) in the Pacific Northwest of North America. Western Washington University Masters Thesis Collection. Paper 185.

Smith, L.P. and C.W. Stockton, 1981. Reconstructed Streamflow for the Salt and Verde Rivers from Tree-Ring Data. Water Resources Bulletin 17:939-947.

Speer, J.H., T.W. Swetnam, B.E. Wickman, and A. Youngblood, 2001. Changes in Pandora Moth Outbreak Dynamics During the Past 622 Years. Ecology 82:679-697.

St. George, S. and T.R. Ault, 2014. The Imprint of Climate within Northern Hemisphere Trees. Quaternary Science Reviews 89:1-4.

Tohver, I., A.F. Hamlet, and S.Y. Lee, 2014. Impacts of 21st Century Climate Change on Hydrologic Extremes in the Pacific Northwest Region of North America. Journal of the American Water Resources Association 50:1461-1476, DOI: 10.1111/jawr.12199.

Wettstein, J.J., J.S. Littell, J.M. Wallace, and Z. Gedalof, 2011. Coherent Region-, Species- and Frequency-Dependent Local Climate Signals in Northern Hemisphere Tree-Ring Widths. Journal of Climate 24:5998-6012.

Wise, E.K., 2010. Tree Ring Record of Streamflow and Drought in the Upper Snake River. Water Resources Research 46:W11529, DOI: 10.1029/2010WR009282.

Woodhouse, C.A., S.T. Gray, and D.M. Meko, 2006. Updated Streamflow Reconstructions for the Upper Colorado River Basin. Water Resources Research 42:W05415, DOI: 10.1029/2005WR004455.

Woodhouse, C.A. and J.J. Lukas, 2006a. Drought, Tree Rings, and Water Resource Management. Canadian Water Resources Journal 31:297-310.

Woodhouse, C.A. and J.J. Lukas, 2006b. Multi-Century Tree-Ring Reconstructions of Colorado Streamflow for Water Resource Planning. Climatic Change 78:293-315.

Yamaguchi, D.K., 1991. A Simple Method for Cross-Dating Increment Cores from Living Trees. Canadian Journal of Forest Research 21:414-416.